Computers & Geosciences 89 (2016) 44–56

Contents lists available at ScienceDirect

Computers & Geosciences

journal homepage: www.elsevier.com/locate/cageo

Research paper

Developing a reversible rapid coordinate transformation model for the cylindrical projection

Si-jing Ye [a], Tai-lai Yan [b], Yan-li Yue [b], Wei-yan Lin [c], Lin Li [a], Xiao-chuang Yao [a], Qin-yun Mu [c], Yong-qin Li [c], De-hai Zhu [b,*]

[a] Key Laboratory of Agricultural information acquisition technology (Beijing) Ministry of Agriculture, China Agricultural University, Beijing 100083, China
[b] Key Laboratory of Agricultural Land Quality (Beijing) Ministry of Land and Resources, China Agricultural University, Beijing 100083, China
[c] Geographic Information Systems Research Center, Feng Chia University, Taichung, Taiwan

ARTICLE INFO

Article history:
Received 19 December 2014
Received in revised form
21 September 2015
Accepted 15 January 2016
Available online 19 January 2016

Keywords:
Inverse transformation
Forward transformation
Numerical models
Map projection
Geographic information systems

ABSTRACT

Numerical models are widely used for coordinate transformations. However, in most numerical models, polynomials are generated to approximate "true" geographic coordinates or plane coordinates, and one polynomial is hard to make simultaneously appropriate for both forward and inverse transformations. As there is a transformation rule between geographic coordinates and plane coordinates, how accurate and efficient is the calculation of the coordinate transformation if we construct polynomials to approximate the transformation rule instead of "true" coordinates? In addition, is it preferable to compare models using such polynomials with traditional numerical models with even higher exponents? Focusing on cylindrical projection, this paper reports on a grid-based rapid numerical transformation model – a linear rule approximation model (LRA-model) that constructs linear polynomials to approximate the transformation rule and uses a graticule to alleviate error propagation. Our experiments on cylindrical projection transformation between the WGS 84 Geographic Coordinate System (EPSG 4326) and the WGS 84 UTM ZONE 50N Plane Coordinate System (EPSG 32650) with simulated data demonstrate that the LRA-model exhibits high efficiency, high accuracy, and high stability; is simple and easy to use for both forward and inverse transformations; and can be applied to the transformation of a large amount of data with a requirement of high calculation efficiency. Furthermore, the LRA-model exhibits advantages in terms of calculation efficiency, accuracy and stability for coordinate transformations, compared to the widely used hyperbolic transformation model.

1. Introduction

Generally, the geographic coordinate system and the plane coordinate system are two basic coordinate systems in spatial data storage and expression. Geoscience data obtained by global positioning systems (GPS), which is the most popular surveying technique used in the determination of geodetic networks, are expressed with reference to geographic coordinates. In contrast, spatial data applied in various industries (e.g., transportation, land resource management) across many countries are referenced to plane coordinate systems. Therefore, in many data integration applications, the original spatial data that users obtain are not unified in the same coordinate system and a projection transformation between geographic coordinates and plane coordinates is necessary (Zhongming et al., 2013).

On the premise of not involving a coordinate reference datum transformation, a projection transformation can be performed by two styles of models: analytical models and numerical models. Analytical models implement a forward transformation and an inverse transformation according to a complex nonlinear functional relation between the specific geographic coordinate system and the plane coordinate system (Zhizhuo, 1990) and have advantages in terms of accuracy compared to numerical models. However, the analytical model is not applicable in all circumstances, e.g., when reference ellipsoid parameters are unknown or the analytic projection equations do not exist (Ipbuker, 2002). Although many approaches to improving execution efficiency have been proposed, such as using a trigonometric series and Clenshaw summation (Engsager, 2007), skipping the calculation of the convergence and scale (Karney, 2011), and applying differential operator theory (Liucheng, 2013) or complex-variable functions (Bowring, 1990), analytical models remain inapplicable in certain

* Correspondence to: Tsing Hua East Road No.17, Beijing 100083, China.
E-mail addresses: b1211682@cau.edu.cn (S.-j. Ye), 610628289@qq.com (D.-h. Zhu).

http://dx.doi.org/10.1016/j.cageo.2016.01.007
0098-3004/

cases that require high calculation efficiency, e.g., spatial data integration, where a substantial amount of geographic coordinate system-based spatial data must be quickly projected to the plane coordinate system for calculation or display purposes. Numerical transformation models, which use control points to construct a polynomial approximation of theoretical coordinates, exhibit various advantages, such as high efficiency and wide versatility, without specifically referencing ellipsoid parameters, and they have been widely used in the aforementioned situations (Yang and Snyder, 2000). Several universal polynomials are applied in numerical models: binary quadratic equations, binary cubic equations, biquadratic interpolation equations, etc. As shown experimentally, the form and degree of the polynomial, together with the distribution and quantity of control points and the transformation area, influence the accuracy and stability of the projection transformation (Yang and Snyder, 2000). On this basis, constructing an appropriate numerical algorithm according to the characteristics of the calculation area or the actual requirements of accuracy and efficiency and thereby realizing an excellent engineering application become an important problem to be solved. SUN Weixin et al. demonstrate that a quadratic orthomorphic polynomial is more appropriate than a binary cubic polynomial and a biquadratic interpolation polynomial for the inverse transformation of a Gauss projection by comparing their calculation precision and stability (Weixin et al., 2013). The experiment also shows that the least square method is more accurate than the direct solution method in terms of solving for these aforementioned polynomials. Hardy proposes a global multi-quadratic transformation model and provides a detailed overview of its applications in geodesy, geophysics, surveying, mapping, photogrammetry, remote sensing, signal processing, geography, digital terrain models and hydrology (Hardy, 1990). Nevertheless, the accuracy of these numerical models is sensitive to the distribution and quantity of control points. Cromley proposes a hyperbolic transformation consisting of two shortened, second-order polynomials and reduces the error uncertainty induced by control points through the use of a graticule to split the transformation area (Cromley, 1991). In this approach, each quadrangle of the graticule is handled as an independent unit, and its four vertexes are used as control points to solve for the polynomial coefficients. On this basis, Ozaki et al. improve the solution efficiency of the hyperbolic function for inverse coordinate transformations using each variable separately in the approximation process (Ozaki et al., 2005). Qi et al. apply Cromley's model on a raster map projection transformation and prove that this model not only satisfies the precision demand but also greatly improves transformation speed (Qi et al., 2002). Bildirici compares Cromley's model with Hardy's model for inverse transformations and concludes that the former model delivers more accurate results (Bildirici, 2003). Xie proposes a MULTI-RANK model in which the parametric solution of a first-order hyperbolic polynomial is amended by cubic and quadratic polynomials (Xie, 2011). Junhua et al. provide a bi-directional iteration algorithm for inverse transformations based on an analysis of the transformation rule between geographic coordinates and plane coordinates (Junhua et al., 2004). On that basis, a variety of strategies using computing clusters or GPU have been developed to accelerate the projection of large geospatial data sets (Behzad, 2012; Finn, 2012). Jenny gives a recent glimpse at some of these studies and demonstrates high-performance projection of raster data in web browsers based on WebGL (Web Graphics Library) (Jenny, 2015). However, in most numerical models, polynomials are used to fit the approximate numerical relationship between geographic coordinates and their corresponding plane coordinates in a local region, without considering the "transformation rule" (or geometric characteristic) of coordinate transformation. As there is a transformation rule between geographic coordinates and plane coordinates, how accurate and efficient is the calculation if we construct polynomials to approximate the transformation rule instead of "true" coordinates?

This paper reports on a grid-based rapid numerical transformation model – a linear rule approximation model (LRA-model) for cylindrical projection transformation, which forms linear polynomials to approximate the transformation rule and uses a graticule to alleviate error propagation. Our experiments on a cylindrical projection transformation between the WGS 84 Geographic Coordinate System (EPSG 4326) and the WGS 84 UTM ZONE 50N Plane Coordinate System (EPSG 32650) with simulated data demonstrate that the LRA-model is comparatively simple and stable for any point in space, although it does not exclude systematic errors due to imperfections in defining the reference ellipsoid. Furthermore, the LRA-model is appropriate for both forward and inverse transformations simultaneously because the inverse equations can be easily derived, and the computational costs and errors can be reduced compared to the hyperbolic model.

The remainder of the article is organized as follows: Section 2 provides the details of the LRA-model, including its principles, polynomials and application process. Section 3 reports on related experiments using the LRA-model on both forward and inverse transformations between the WGS 84 Geographic Coordinate System (EPSG 4326) and the WGS 84 UTM ZONE 50N Plane Coordinate System (EPSG 32650) with simulated data in three zones with different latitudes. In addition, this section provides a detailed comparison between the LRA-model and the hyperbolic model in terms of accuracy, efficiency and stability. Finally, Section 4 discusses and concludes this study. The accuracy and stability of the LRA-model on azimuthal or conic projections will be tested in future research.

2. Linear rule approximation model

2.1. Methodology and model development

The earth can be approximated as a rotational ellipsoid, and on this basis, we can treat "circles" of longitude as a set of ellipses that share the same semi-major axis, semi-minor axis and symmetry axis while treating "circles" of latitude as concentric "circles" with different radii. Lines of latitude and longitude on the ellipsoid surface are continuous and inerratic curves, and their corresponding projection coordinates are continuous, finite and single valued in the cartographic region; otherwise the map projection is meaningless. "Circles" of longitude and "circles" of latitude are very large, even at high latitudes, and they can be approximated as straight lines in a small local region. In addition, this trend remains if we project these two types of "circles" onto a plane map. Moreover, the international map subdivision of basic scale topographic maps generally uses partial lines of latitude and longitude as borders. On one side of the meridian in the Northern Hemisphere, any two arbitrary latitude lines can split longitude lines into "innumerable" line segments, with the slope of the line segments relative to the meridian increasing as the distance from the meridian increases. Similarly, latitude lines can be split bay any two arbitrary longitude lines, with the slope of the line segment relative to the equator increasing as the distance from the equator increases. The slopes of latitude line segments (relative to the equator) and of longitude line segments (relative to meridian) vary in the same manner. Therefore, there is an approximate linear relation between geographic coordinates and plane coordinates using the premise that the transformation region is sufficiently small.

Fig. 1 presents the principle of the projection transformation

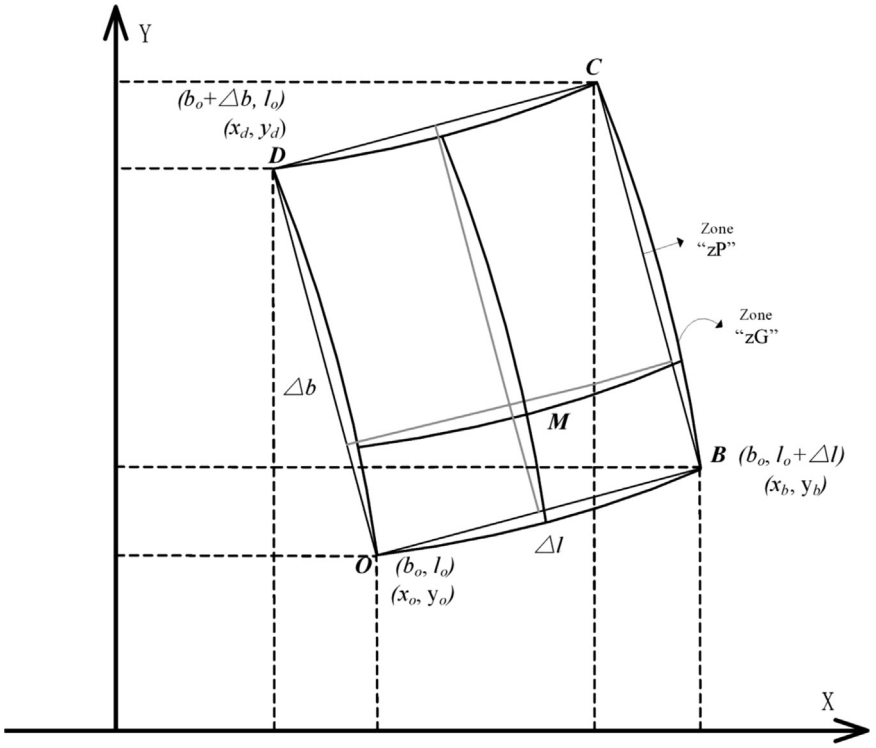

Fig. 1. Principle of projection transformation based on the Universal Transverse Mercator (UTM) projection.

base on the Universal Transverse Mercator (UTM) projection. *X* and *Y* represent the axis of the Plane Coordinates System; the *X*-axis points to the east and overlaps with the equator, and the *Y*-axis points to the north and overlaps with the central meridian. Projection distortion is symmetrical about the equator and central meridian with respect to the partial lines of latitude and longitude and intensifies with increasing distance to the central meridian or the equator. As shown in Fig. 1, zone "zG" is a small projection transformation region enclosed by a line of latitude and longitude on the ellipsoid surface. Δl and Δb are the longitudinal extent and latitudinal extent of zone "zG"; therefore, the four vertexes of the geographic coordinates of "zG" can be expressed as O (b_o, l_o), B $(b_o, l_o+\Delta l)$, C $(b_o+\Delta b, l_o+\Delta l)$ and D $(b_o+\Delta b, l_o)$, where "*b*" represents latitude and "*l*" represents longitude. Zone "zP", an approximately rectangular region, is the corresponding projection of "zG" on a plane map ("zG" and "zP" are not on the same level). For a representative point in zone "zG", the change in latitude is the main factor for the change in the *y* coordinate, and the *x* coordinate mainly responds to a change in longitude during the projection transformation process. In spite of being influenced by both latitude and longitude, the variation characteristics of the *y* coordinate and *x* coordinate are mainly controlled by the latitude and longitude, respectively. With the continuous decreasing of Δl and Δb, the segmental arcs OB and OD asymptotically approach a straight line, and each edge of both zone "zG" and zone "zP" is nearly parallel to its opposite side. In this case, set point O as the original point, and for any point M(b_m, l_m) in zone "zG", the relation between the increment of latitude (b_m-b_o) and longitude (l_m-l_o) corresponding to the geographic coordinate of point O(b_o, l_o) and the increment of the x/y coordinate to the plane coordinate of point O(x_o, y_o) tends to be constantly linear. On this basis, we have constructed simple polynomials to approximate this linear relation for the forward transformation, as shown in Eq. (1).

$$\begin{cases} x=x_o+\partial_L(l-l_o)+\partial_B(b-b_o) \\ y=y_o+\theta_B(b-b_o)+\theta_L(l-l_o) \end{cases} \quad (1)$$

According to Eq. (1), (x, y) and (b, l) represent the plane coordinates and geographic coordinates of the point being transformed, respectively, while (x_o, y_o) and (b_o, l_o) are the plane coordinates and geographic coordinates of the original point O, respectively. ∂_L, ∂_B, θ_B and θ_L represent undetermined transformation coefficients, where ∂_L and θ_B are primary coefficients that play an important role in constructing the proportional relation between the two different aforementioned coordinate systems. ∂_B and θ_L are auxiliary coefficients: ∂_B is set to smooth the fluctuation of the y coordinate caused by the curling of the latitude line with increasing longitude, and θ_L is set to adjust the variation in the *x* coordinate caused by the convergence of the longitude line with increasing latitude. ∂_L and θ_B are much larger than ∂_B and θ_L. In a coordinate transformation region such as zone "zG", because of the geographic coordinates of the original point O, the longitudinal extent (Δl) and latitudinal extent (Δb) are known, and the equations for ∂_L, ∂_B, θ_B and θ_L can be easily derived, as shown in Eq. (2).

$$\begin{cases} \partial_L=\dfrac{(x_b-x_o)}{\Delta l} \\ \partial_B=\dfrac{(x_d-x_o)}{\Delta b} \\ \theta_L=\dfrac{(y_b-y_o)}{\Delta l} \\ \theta_B=\dfrac{(y_d-y_o)}{\Delta b} \end{cases} \quad (2)$$

The plane coordinates of O$(x_o,\ y_o)$, B$(x_b,\ y_b)$ and D$(x_d,\ y_d)$ are previously calculated according to the traditional analytical model for projection transformations. These undetermined transformation coefficients can be calculated by substituting the plane coordinates of point O, B and D into Eq. (2), which also illustrates that the LRA-model cannot be more accurate than the traditional analytical model. Furthermore, Eq. (3) can be easily derived from

Eq. (1) for the inverse transformation.

$$\begin{cases} l=l_o+\partial_x(x-x_o)+\partial_y(y-y_o) \\ b=b_o+\theta_y(y-y_o)+\theta_x(x-x_o) \end{cases} \quad (3)$$

Any point in zone "zG" (or zone "zP") is appropriate in the LRA-model for projection transformations. We stress that both the four undetermined transformation coefficients and the coordinates of the original point O vary with location and with the spatial span of the coordinate transformation region. In other words, each coordinate transformation region corresponds to a set of coefficients, which can be calculated according to the location and spatial span of the region. In addition, the spatial span, including longitudinal extent (Δl) and latitudinal extent (Δb), is one of the most critical factors in the transformation error. If the original point O is determined, the transformation error decreases as Δl and Δb decrease, following a complicated functional relation. Furthermore, error fluctuations among different locations of the transformation region cannot be described as a simple linear distribution. It is important to note that, although Eqs. (1) and (3) are similar to affine transformation in the expression format, they are deduced based on our assumption that the increment of geographic coordinates has an approximate linear relationship with the increment of plane coordinates both lengthwise and crosswise and can address some problems that affine transformation cannot, e.g., identifying where homonymy points should be deployed.

2.2. Grid-based model implementation

The LRA-model has the advantages of high computational efficiency, ease of use and simple form because projection transformations are performed using linear polynomials. However, because these polynomials are only suitable for a small transformation region, how can they be applied to larger areas with the condition of maintaining a stable error? To solve this problem, we have referenced grid generation theory, alleviated error propagation and maintained a stable error using equally spaced lines that split the entire transformation region into a set of small "rectangle" grids distributed in the form of rows and columns. Fig. 2 presents details of the generation of the "rectangle" grids for forward transformations. In this model, each grid is addressed as an independent unit. The latitude and longitude of the four vertexes, together with their relevant plane coordinates, are known for each grid.

The LRA-model is visually described in Fig. 3. First, the entire transformation region has been divided into a set of grids by equally spaced lines, whose interval distance is determined by the accuracy demands of the specific application. Then, for each grid, the vertex with the minimum latitude and longitude is set as the original point, and the plane coordinates of the vertices are determined using the traditional analytical model. On this basis, the original point of each grid, and the longitudinal and latitudinal extent, is used to compute transformation coefficients and construct linear transformation polynomials. Then, all coefficients are imported to a relational database table, whose structure is shown in Table 1. Finally, for any point to be transformed in the region, the grid that contains it is sought. The point is then transformed using the coefficients of the unit that contains it.

In this situation, the efficiency of seeking the grid container and extracting coefficients significantly impacts the computational efficiency of the LRA-model. A grid encoding method has been used to reduce the time spent on database interaction. As shown in Fig. 2, each grid is encoded in the form of "row number_column number". Thus, the grid in the southwest corner of the entire transformation region is assigned an initial encoding grid with code "0_0". Then, the row number and column number continuously increase by one in the y direction and x direction, respectively. Therefore, the code of the grid that contains the point to be transformed can be directly calculated according to Eq. (4). We use a simulated point M in the region as an example, where b'_m and l'_m represent the latitude and longitude of M, respectively, while the geographical coordinates for the original point of the initial encoding grid are expressed as b'_o and l'_o. $\Delta l'$ represents the

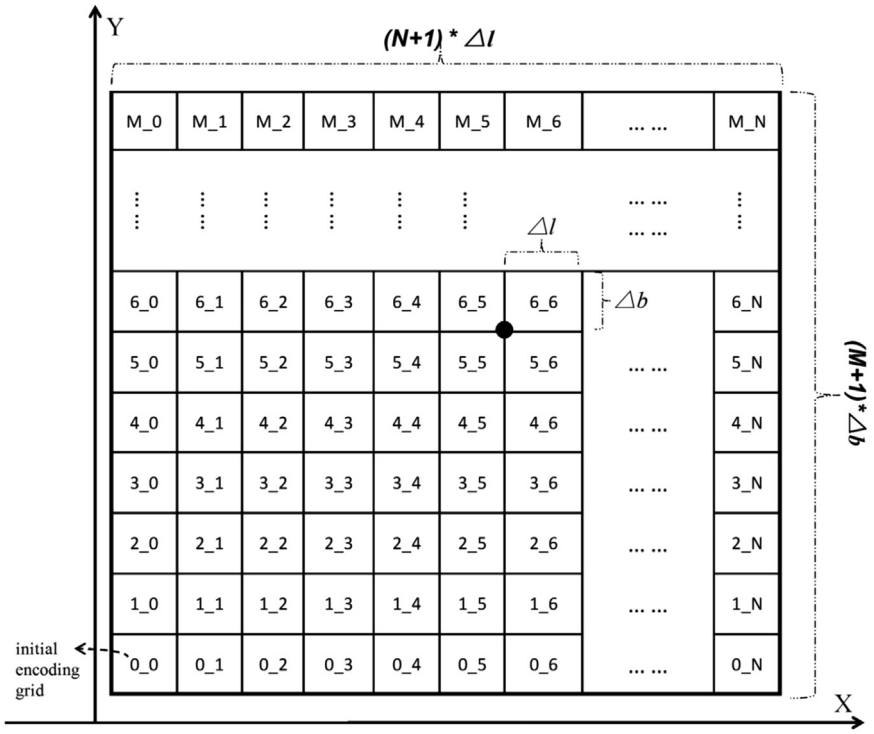

Fig. 2. Details of grid generation for forward transformation.

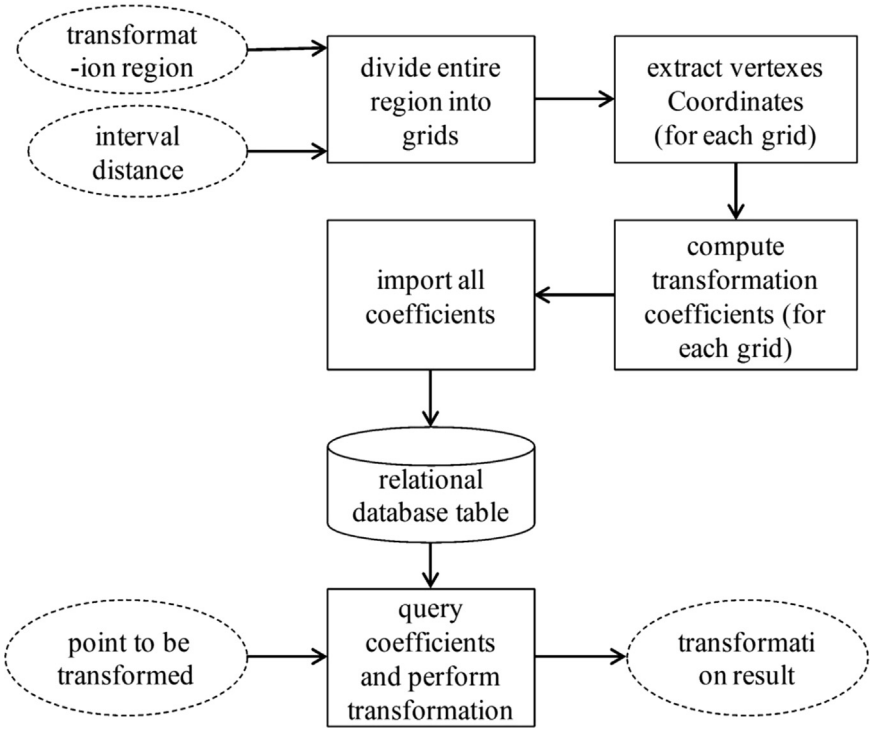

Fig. 3. LRA-model process.

Table 1
Structure of data table for storing transformation coefficients.

Grid Code	Original Point Latitude (b_o)	Original Point Longitude (l_o)	Original Point X (x_o)	Original Point Y (y_o)	∂_L	∂_B	θ_L	θ_B
0_0								
…	…	…	…	…	…	…	…	…
M_N								

longitudinal extent, and $\Delta b'$ represents the latitudinal extent. "[ ]" is used to round down the result to the nearest integer. N_B and N_L represent the row number and column number, respectively, and the code of the grid that the point M belongs to is "N_B_N_L". It is important to note that, in our experiments, b'_m, l'_m, b'_o, l'_o, $\Delta b'$ and $\Delta l'$ can appropriately be measured in minutes (′). For instance, "120°20′"(longitude) is expressed as "7220′".

$$\begin{cases} N_B = \left[\dfrac{b'_m - b'_o}{\Delta b'} \right] \\ N_L = \left[\dfrac{l'_m - l'_o}{\Delta l'} \right] \end{cases} \quad (4)$$

Supported by this grid generation and encoding strategy, the LRA-model can be applied to a large area for both forward and inverse transformations on the premise of maintaining stable errors. In addition, for practical applications, the transformation error can be limited to meet the specific accuracy requirements by adjusting the interval distance of the equally spaced lines.

3. Experiments and analysis

3.1. Experimental environment and data

Our experiments are all performed using a transformation between the WGS 84 Geographic Coordinate System (EPSG 4326) and the WGS 84 UTM ZONE 50N Plane Coordinate System (EPSG 32650) in three zones with different latitudes. Because the distortion of the UTM projection is symmetrical around the equator and central meridian, we deploy all of the three zones on the same side of these two symmetry axes. Fig. 4(1) presents the experimental transformation zones in the geographic coordinate system for forward transformations. The horizontal axis indicates the longitude, and the vertical axis indicates the latitude. Zone "zG1", "zG2" and "zG3" share the same longitudinal extent (3°) and latitudinal extent (3°), and the geographic coordinates of their southwest corner are (114°, 24°), (114°, 34°) and (114°, 44°), respectively. To analyze the error distribution, 3,240,000 simulated points have been evenly deployed in each zone for the forward transformation experiment. The distance between adjacent points is 0.1'. Fig. 4(2) presents the experimental transformation zones in the plane coordinate system for the inverse transformation. Zones "zP1", "zP2" and "zP3" share the same length (300 km) and width (220 km), and there are 6,600,000 simulated points evenly distributed in each zone at an interval of 0.1 km.

Using the same computer language (C#), a traditional analysis model based on a truncated series (TS-model) has been implemented to transform the simulated points, and the transformation results are considered as "truth values" for the error calculation. All the experiments have been performed on a single thread in the same software and hardware environment, as shown in Table 2.

3.2. LRA-model validation

First, during our forward transformation process (Fig. 4(1)), grids with the same size have been generated in zones "zG1", "zG2" and "zG3". Both the longitudinal extent and latitudinal extent have been set to 0.5′. Because the number of points and grids are the same in each zone, we have tested the time elapsed in the LRA-model by transforming 3,240,000 points only in zone "zG1". A traditional analytical model (Karney, 2011) based on a truncated series (TS-model) was implemented in.NET for comparison. For a

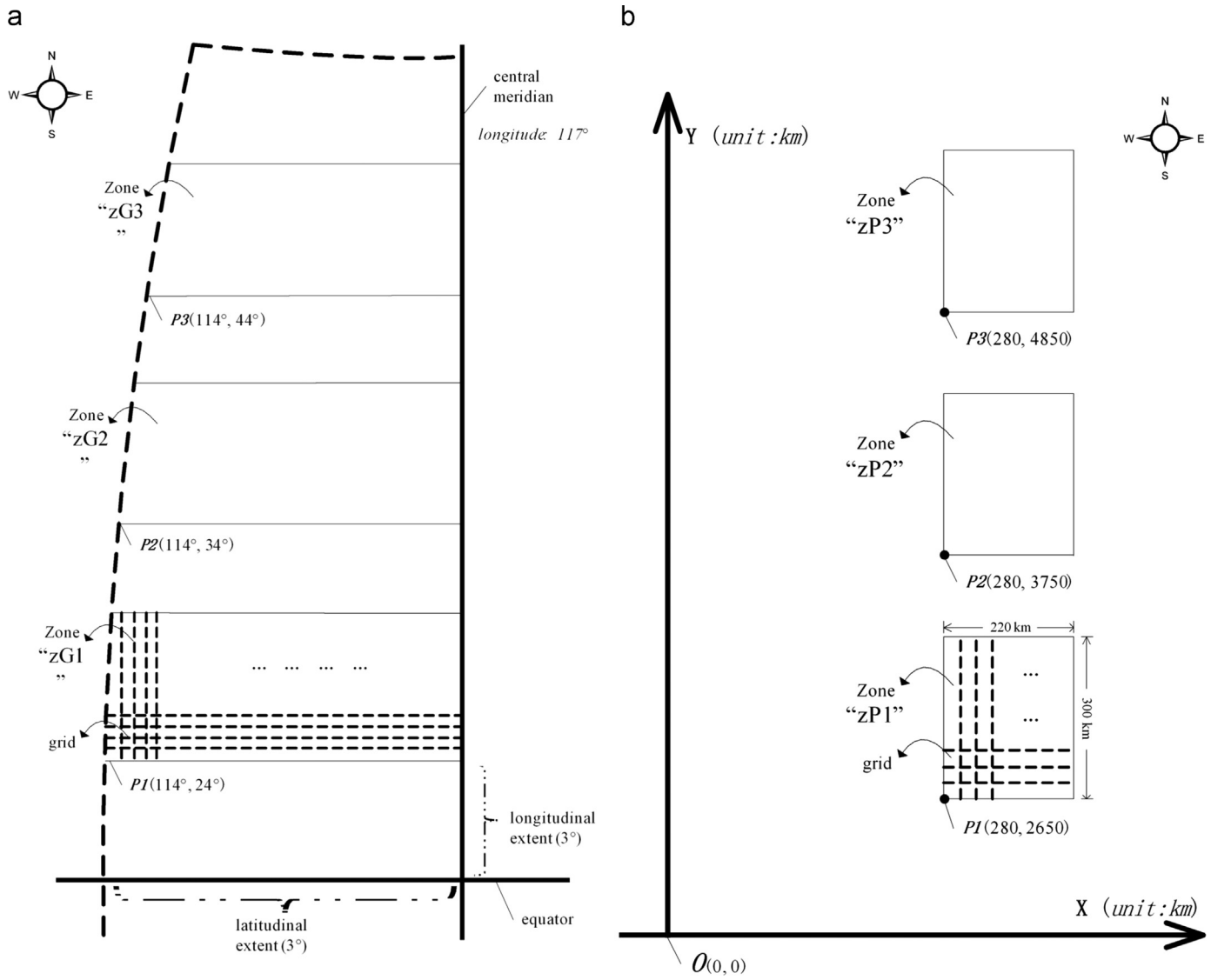

Fig. 4. (1) Experimental transformation zones for forward transformation, (2) Experimental transformation zones for inverse transformation.

Table 2
Software and hardware environment for the experiments.

Parameter name	Parameter values
central processing unit	Intel Core i7-4900MQ @2.8 GHz (4 cores)
internal storage	16 GB (SUMSUNG DDR3L 1600 MHz)
video memory	4 GB (NVIDIA GeForce GTX 780 M)
operating system	Windows 7 SP1 × 64
development platform	Microsoft Visual Studio 2012
programming language	C#

point with latitude $\boldsymbol{b}$, longitude $\boldsymbol{l}$ and corresponding UTM plane coordinates x and y, the transformation formula for the TS-model is shown in Eq. (5). $E_o=500$ km and $N_o=0$ km in the Northern Hemisphere. The scale on the central meridian $k_o=0.9996$. $A,\alpha_1, \alpha_2\ldots$ can be solved using Eqs. (8) and (9). $2\pi A$ is the circumference of a meridian; $\mathbf{a}$ represents the equatorial radius ($\mathbf{a}$=6378. 137km) and $\boldsymbol{n}$ represents third flattening ($\boldsymbol{n}=\frac{f}{2-f}$, with inverse flattening of $\frac{1}{f}$=298. 257223563). The first eccentricity is represented by $\boldsymbol{e}=\sqrt{\frac{f}{2-f}}$. Because the ellipsoidal parameters are known, $A,\alpha_1, \alpha_2\ldots,\mathbf{a},\boldsymbol{n}, \boldsymbol{e}$ can be treated as constants in the experiment. The solutions for η' and ξ' are shown in Eq. (6), where $\acute{\tau}$ can be figured out using Eq. (7).

$$\begin{cases} x=E_o+k_oA\left(\eta'+\sum_{j=1}^{4}\alpha_j\cos(2j\xi')\sinh(2j\eta')\right) \\ y=N_o+k_oA\left(\xi'+\sum_{j=1}^{4}\alpha_j\sin(2j\xi')\cosh(2j\eta')\right) \end{cases} \tag{5}$$

$$\begin{cases} \eta'=\sinh^{-1}\left(\frac{\sin(l)}{\sqrt{\acute{\tau}^2+\cos l^2}}\right) \\ \xi'=\tan^{-1}\left(\frac{\acute{\tau}}{\cos l}\right) \end{cases} \tag{6}$$

$$\acute{\tau}=(\tan b)\sqrt{1+\delta^2}-\delta\sqrt{1+(\tan b)^2}$$

$$\delta=\sinh\left(e\tanh^{-1}\left(\frac{e\tan b}{\sqrt{1+(\tan b)^2}}\right)\right) \tag{7}$$

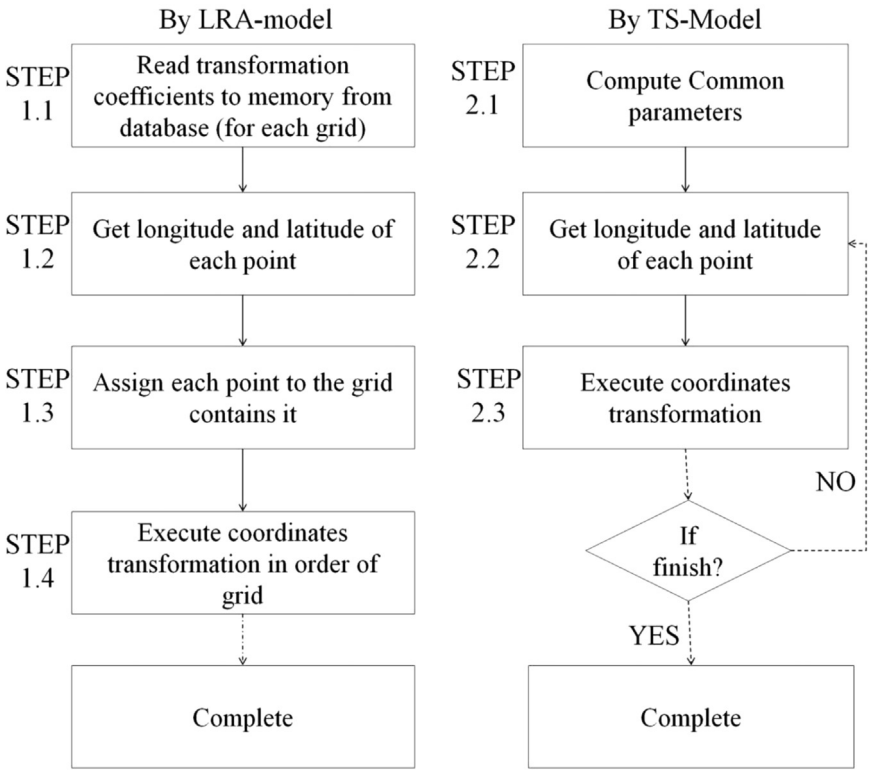

Fig. 5. Coordinates transformation process of the LRA-model and the TS-model.

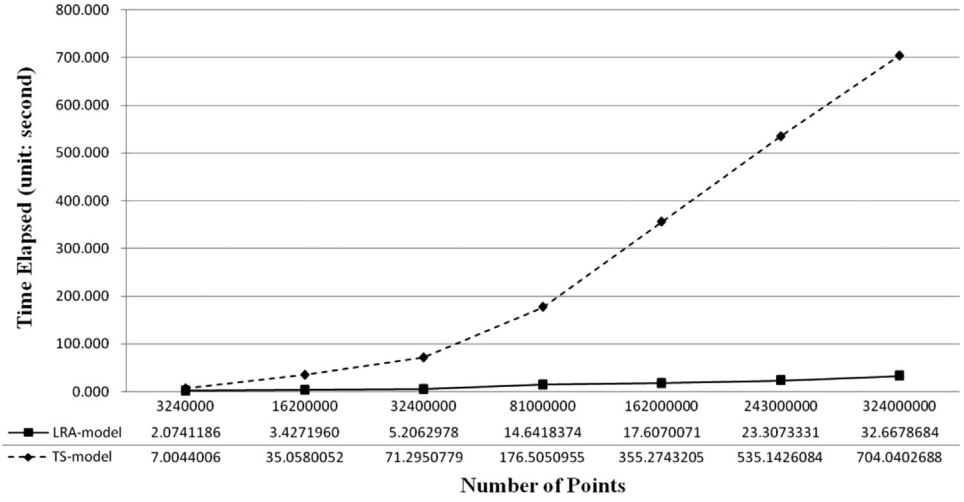

Fig. 6. Computational time of the LRA-model compared to the TS-model.

Table 3
Maximum error and RMSE of the LRA-model implemented in zones with different latitudes (for forward transformations).

zone	MaxED[a]	MaxEX[b]	MaxEY[c]	RMSE[d]
zG1	0.4735802	0.4231424	0.2387306	0.1014944
zG2	0.5142580	0.4087437	0.3386037	0.0943728
zG3	0.5769861	0.3830936	0.4639421	0.1021926

[a] Maximum distance error (unit: meter).
[b] Maximum absolute error in the *X* direction (unit: meter).
[c] Maximum absolute error in the *Y* direction (unit: meter).
[d] RMSE for distance (unit: meter).

$$\begin{cases} \alpha_1=\frac{1}{2}n-\frac{2}{3}n^2+\frac{5}{16}n^3+\frac{41}{180}n^4 \\ \alpha_2=\frac{13}{48}n^2-\frac{3}{5}n^3+\frac{557}{1440}n^4 \\ \alpha_3=\frac{61}{240}n^3-\frac{103}{140}n^4 \\ \alpha_4=\frac{49561}{161280}n^4 \end{cases} \tag{8}$$

$$A=\frac{a}{1+n}\left(1+\frac{1}{4}n^2+\frac{1}{64}n^4+\frac{1}{256}n^6\right) \tag{9}$$

The experiment process is shown in Fig. 5. For the TS-model, longitude and latitude for each point can be obtained and transformed one by one by computing common parameters such as

Table 4
Maximum error and RMSE of the LRA-model implemented in zones with different latitudes (for inverse transformations).

Zone	Model	MLONE[a]	RMSELON[b]	MLATE[c]	RMSELAT[d]
zP1	LRA-model	2.7139009E-04	6.6824057E-05	6.4260925E-05	1.6770557E-05
zP2	LRA-model	2.9903019E-04	6.8300955E-05	1.1839086E-04	3.0919979E-05
zP3	LRA-model	3.1504516E-04	7.1717205E-05	1.2816153E-04	3.3546185E-05

[a] Maximum longitude error (unit: minute (′)).
[b] RMSE for longitudes (unit: minute (′)).
[c] Maximum latitude error (unit: minute (′)).
[d] RMSE for latitudes (unit: minute (′)).

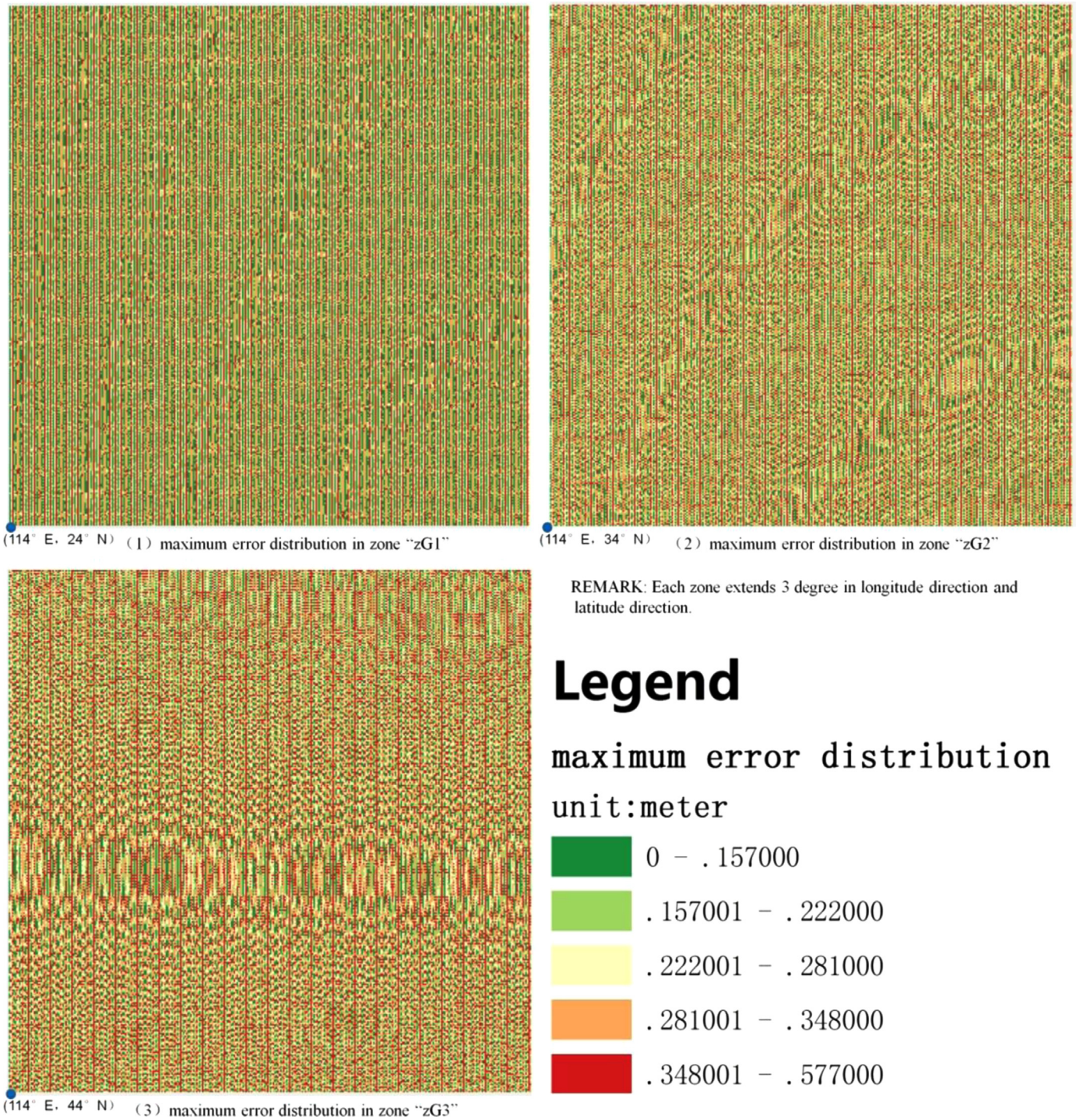

Fig. 7. Grid-based maximum distance error distribution in different zones (forward transformation).

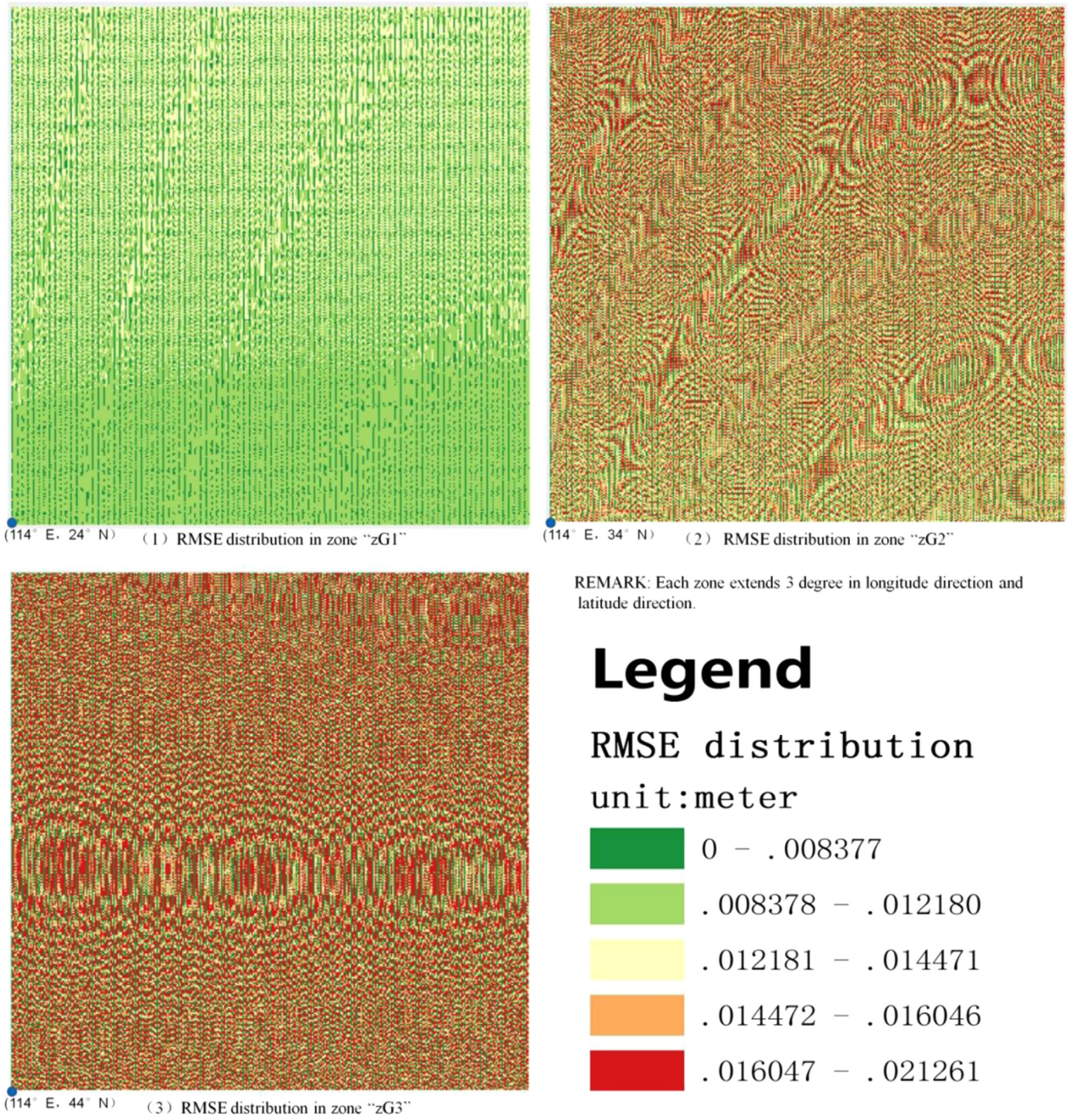

Fig. 8. Grid-based RMSE distribution in different zones (forward transformation).

A,α_1, α_2…. In contrast, for the LRA-model, transformation coefficients of each grid have been read to memory, and each point has been assigned to the grid to which it belongs before batch transformation. All the points are then transformed by grid order. In this manner, points belonging to the same grid can be transformed with uniform coefficients, and time spent on querying coefficients can be reduced. To exhibit the performance difference, the number of points has been expanded to 16,200,000, 32,400,000, 81,000,000, 162,000,000, 243,000,000, and 324,000,000 by replicating all the simulated points (3,240,000) 5 times, 10 times, 25 times, 50 times, 75 times and 100 times. The test results are shown in Fig. 6.

Then, the coordinate transformation has been performed on each point of the three zones, and the maximum error (unit: meter) and RMSE of each zone has been recorded to illustrate whether the LRA-model is applicable in regions with different latitudes, as shown in Table 3.

Similar strategies have been used to validate the applicability of the LRA-model for inverse transformations (Fig. 4(2)). 1*1 km grids have been generated in zones "zP1", "zP2" and "zP3". For each zone, the LRA-model has been used to transform 6,600,000 simulated points from the plane coordinate system to the

Table 5
Variation characteristics of computation time and maximum error with changing grid size.

Zone	grid size	TC[a]	MaxED[b]	MaxEX[c]	MaxEY[d]
zG1	0.5′	2.0741186	0.4735802	0.4231424	0.2387307
	1′	0.8500011	0.6225080	0.5899268	0.2657897
	2′	0.5600008	1.3083931	1.2959844	0.3643282
	3′	0.5000007	2.4431605	2.4384060	0.5338135
	4′	0.4100006	4.1773930	4.1598720	0.7868930
	5′	0.3700002	6.2640316	6.2534498	1.0722386
	6′	0.3080169	8.9787608	8.9625323	1.5101576
	9′	0.3020176	19.8785998	19.8515265	3.0491954
	10′	0.3360187	24.4576273	24.4188515	3.7770157

[a] Time elapsed (unit: second).
[b] Maximum distance error (unit: meter).
[c] Maximum absolute error in the *X* direction (unit: meter).
[d] Maximum absolute error in the *Y* direction (unit: meter).

Table 6
Differences in computation time, maximum error and RMSE between the LRA-model and the HT-model for forward transformations.

Zone	Model	TC[a]	MaxED[b]	MaxEX[c]	MaxEY[d]	RMSE[e]
zG1	LRA-model	2.0741186	0.4735802	0.4231424	0.2387306	0.1014944
	HT-model	2.1700027	1.1226630	1.1224094	0.1195130	0.2224501
zG2	LRA-model	–	0.5142580	0.4087437	0.3386037	0.0943728
	HT-model	–	1.9022587	1.9022587	0.1656884	0.2962586
zG3	LRA-model	–	0.5769861	0.3830936	0.4639421	0.1021926
	HT-model	–	1.9935788	1.9860823	0.2135783	0.3620850

[a] Time elapsed (unit: second).
[b] Maximum distance error (unit: meter).
[c] Maximum absolute error in the *X* direction (unit: meter).
[d] Maximum absolute error in the *Y* direction (unit: meter).
[e] RMSE for distance (unit: meter).

geographic coordinate system. Table 4 expresses the maximum error (unit: minute) and RMSE of each zone.

As shown in Tables 3 and 4, the LRA-model is stable, convergent and easy to implement and also exhibits significantly higher coordinate transformation efficiency compared to traditional analytical models. In the forward transformation process between the WGS 84 Geographic Coordinate System and the WGS 84 UTM ZONE 50N Plane Coordinate System, the error can be limited to less than 0.5769862 m across the area at a latitude of less than 47° (Northern Hemisphere) and a longitude between 114° and 120° (Eastern Hemisphere) based on grids with an interval distance of 0.5′. The maximum distance error increases with increasing latitude, and this change is mainly caused by the error in the *Y* direction because the maximum absolute error in the *X* direction tends to decrease, and there is no obvious relation between the RMSE and the latitude of zones. According to the results of the inverse transformation experiments in a rectangular region with an *x* coordinate between 280,000 and 500,000 (meters) and a *y* coordinate between 2,650,000 and 5,150,000 (meters), the longitude error can be limited to less than 0.00034504517′, and the latitude error can be limited to less than 0.00012816154′. As the transformation zone is located farther north, the better MLONE, MLATE, RMSELON and RMSELAT can be calculated; the MLATE and RMSELAT are smaller but change more dramatically compared to MLONE and RMSELON.

Furthermore, to observe the error distribution regularities, we have referenced the theory of the regionalized variable, where treated points belong to the same grid as a whole, and computed their maximum error and RMSE. On this basis, the error distribution of each zone has been displayed in the form of a two-dimensional image. Using the forward transformation as an example, Fig. 7 presents the maximum error of each grid in zones “zG1”, “zG2” and “zG3”, and Fig. 8 presents their RMSE distribution. The domain of values for classification is defined according to the number of points that belong to it to make the number of points in each domain of values approximately equal. From the perspective of grids, the variation in the maximum error is weakly influenced by the distance from the grid to the equator or central meridian but is distributed based on a special periodic rule. Furthermore, grids located in the same column have a similar maximum error, and this characteristic weakens with increasing latitude. The distribution of the RMSE is clearly influenced by latitude in areas with low latitudes and tends to be smooth with increasing latitude.

Adjusting the longitudinal and latitudinal extent of the grid will affect the accuracy and efficiency of the coordinate transformation. In theory, for transforming a certain number of points, the calculation error will increase as the grid size increases, while the computation time will decrease because the data table records number decreases, thereby increasing the speed of database interaction. We have studied the variation characteristics of the computation time and error with varying grid size. Using a forward transformation in zone “zG1” as an example, grid systems with different interval distances of 0.5′, 1′, 2′, 3′, 4′, 5′, 6′, 9′ and 10′ have been used. Table 5 presents the computation times and the corresponding maximum errors for transforming 3,240,000 points using different grid systems. There is an inverse relation between computation time and grid size, but this relation is weak and fades as the grid size increases. As the grid size increases, MaxED, MaxEX, MaxEY all continuously increase, and their corresponding curves are similar to the curves of exponential functions; namely, the variations become increasingly higher in magnitude. On the

Table 7
Differences in computation time, maximum error and RMSE between the LRA-model and the HT-model for inverse transformations.

Zone	Model	TC[a]	MLONE[b]	RMSELON[c]	MLATE[d]	RMSELAT[e]
zP1	LRA-model	1.430002	2.7139009E-04	6.6824057E-05	6.4260925E-05	1.6770557E-05
	HT-model	1.7900025	2.4553880E-04	6.6447702E-05	8.5798205E-05	2.2236854E-05
zP2	LRA-model	–	2.9903019E-04	6.8300955E-05	1.1839086E-04	3.0919979E-05
	HT-model	–	2.4487138E-04	6.6359297E-05	1.2425255E-04	3.3307111E-05
zP3	LRA-model	–	3.1504516E-04	7.1717205E-05	1.2816153E-04	3.3546185E-05
	HT-model	–	2.5907988E-04	6.6548633E-05	1.5154557E-04	3.9780336E-05

[a] Time elapsed (unit: second).
[b] Maximum longitude error (unit: minute(′)).
[c] RMSE for longitudes (unit: minute(′)).
[d] Maximum latitude error (unit: minute(′)).
[e] RMSE for latitudes (unit: minute(′)).

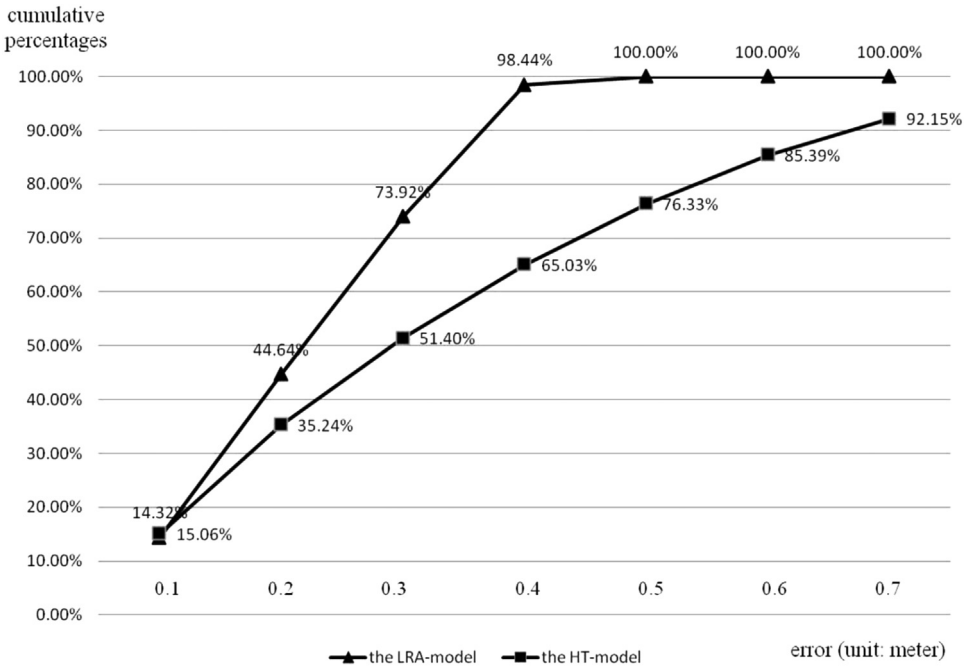

Fig. 9. Number of points within different distance error ranges (forward transformation in "zG1").

premise of keeping the transformation zone unchanged, MaxEX is shown to be more sensitive to changes in grid size; the variation of MaxEX is very similar to that of MaxED, while the variation in MaxEY is smaller and smoother.

3.3. Comparison of models

According to the above experiments, we observe that the LRA-model exhibits high accuracy and speed for both forward and inverse transformations. However, is it preferable to other widely used numerical models for coordinate transformations, or what is the advantage of the LRA-model compared to other numerical models?

In this study, the hyperbolic transformation model (HT-model) proposed by Cromley (1991) has been selected as a representative traditional numerical model because it can be directly solved by four vertices of a "rectangle" grid, and thereby, the error uncertainty induced by control points can be reduced. The HT-model has been widely used for both vector data (Bildirici, 2003; Ozaki et al., 2005) and raster data (Qi et al., 2002); in addition, and most importantly, it is one of the most commonly used models that set up polynomials to approximate "true" geographic coordinates or plane coordinates in a local area.

$$\begin{cases} x=a_1b+a_2l+a_3bl+a_4 \\ y=a_5b+a_6l+a_7bl+a_8 \end{cases} \quad (10)$$

The implementation process of the HT-model is similar to the LRA-model: using equally spaced lines, the entire transformation region is split into a set of small "rectangle" grids distributed in the form of rows and columns, each grid is addressed as an independent unit, and the plane coordinates and geographical coordinates of the four vertices are known for each grid. Two shortened, second-order polynomials are used as forward transformation equations, as shown in Eq. (10). Using four control points, the system (Eq. (10)) can be directly solved, i.e., eight coefficients can be determined. The solution is shown in matrix form in Eq. (11).

$$\underline{A} = \begin{bmatrix} b_1 & l_1 & b_1l_1 & 1 \\ b_2 & l_2 & b_2l_2 & 1 \\ b_3 & l_3 & b_3l_3 & 1 \\ b_4 & l_4 & b_4l_4 & 1 \end{bmatrix},$$

$$\underline{X} = \begin{bmatrix} x_1 & x_2 & x_3 & x_4 \end{bmatrix}^{\mathrm{T}} \quad \underline{Y} = \begin{bmatrix} y_1 & y_2 & y_3 & y_4 \end{bmatrix}^{\mathrm{T}}$$

$$\underline{B} = \begin{bmatrix} a_1 & a_2 & a_3 & a_4 \end{bmatrix}^{\mathrm{T}} \quad \underline{C} = \begin{bmatrix} a_5 & a_6 & a_7 & a_8 \end{bmatrix}^{\mathrm{T}}$$

$$A\underline{B} = \underline{X} \Rightarrow \underline{B} = A^{-1}\underline{X}, \; A\underline{C} = \underline{Y} \Rightarrow \underline{C} = A^{-1}\underline{Y} \quad (11)$$

Because the inverse equations of Eq. (10) are excessively complicated, we have set up Eq. (12) for the inverse transformation.

$$\begin{cases} b=a_1x+a_2y+a_3xy+a_4 \\ l=a_5x+a_6y+a_7xy+a_8 \end{cases} \quad (12)$$

To compare the differences in speed, accuracy and stability between the LRA-model and the HT-model, the HT-model has been applied as a substitute for the LRA-model in both forward and inverse transformations, with the experimental region (Fig. 4), longitudinal/latitudinal extent of each grid (0.5′) and simulated point distribution kept the same as those in the LRA-model validation experiments. Based on the forward transformation result, Table 6 presents the differences in computation time, maximum error and RMSE between these two models in three zones with different latitudes. The computation time, maximum error and RMSE differences found using the inverse transformation are shown in Table 7. Furthermore, cumulative percentage histograms have been used to present the distribution of the point number in different error ranges, as shown in Fig. 9 and Fig. 10.

As shown in Table 6, the LRA-model exhibits higher computation speed and stability compared to the HT-model for forward transformations between the WGS 84 Geographic Coordinate System (EPSG 4326) and the WGS 84 UTM ZONE 50N Plane Coordinate System (EPSG 32650). In each zone, both MaxED and MaxEX can be limited to a significantly smaller range by the LRA-model. Although the HT-model exhibits a higher accuracy in the *Y*

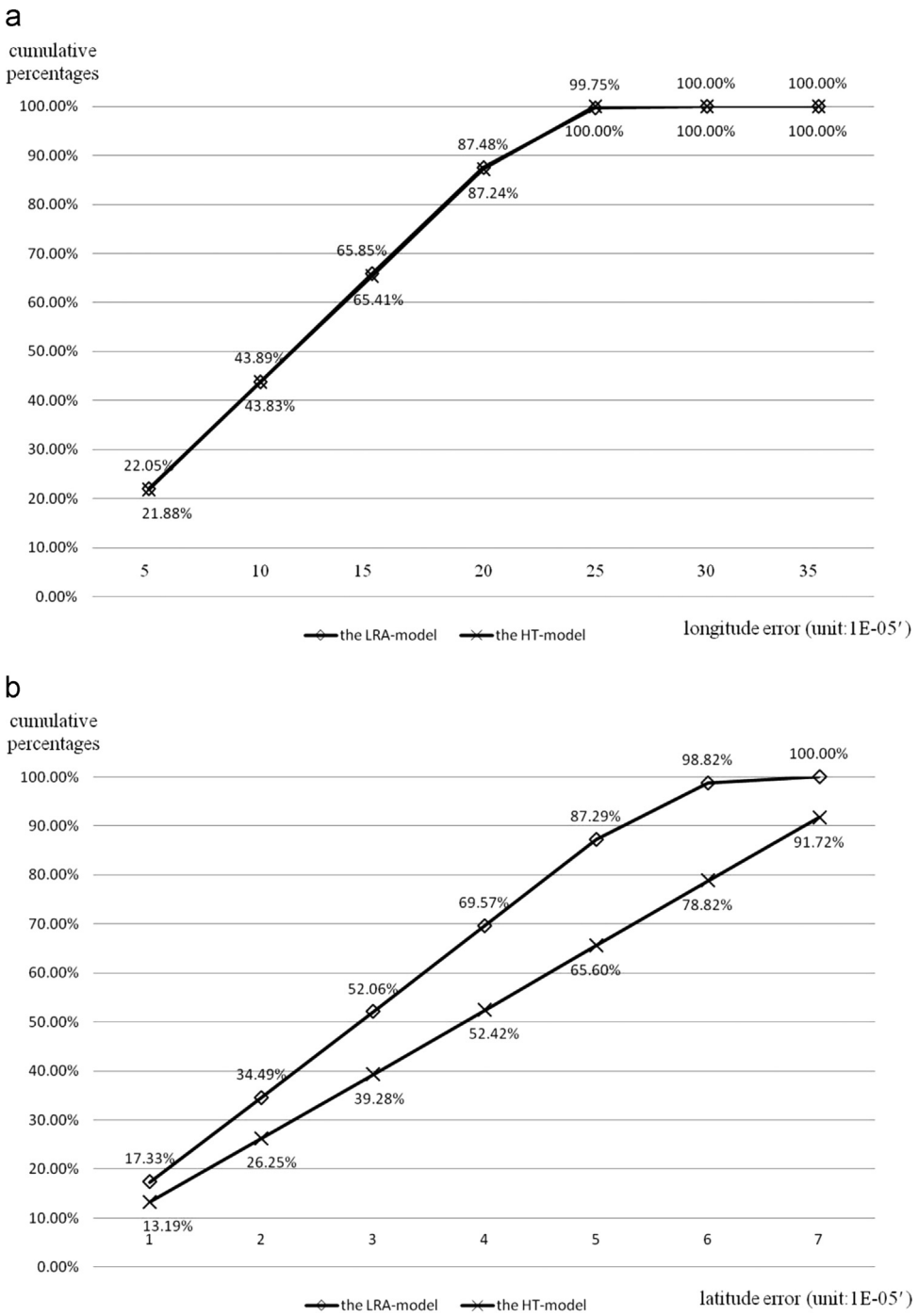

Fig. 10. (1) Number of points within different longitude error ranges (inverse transformation in "zP1"), (2) number of points within different latitude error ranges (inverse transformation in "zP1").

direction (MaxEY), the LRA-model is more homogeneous and more preferable. As shown in Fig. 9, 98.44% of points have a distance error of less than 0.4 m using the LRA-model, while the ratio is only 65.03% for the HT-model.

However, the circumstances change with inverse transformations, as shown in Table 7. First, the LRA-model exhibited a higher computation speed compared to the other model. Second, the choice of model depends on the importance of longitude/latitude error in practical applications because the LRA-model exhibits higher accuracy and stability on latitude transformations, while the HT-model is more preferable for longitude transformations. Third, both of these models have larger errors on longitude transformations. Finally, as shown in Fig. 10, the longitude error distributions of these two models are similar, but the LRA-model is obviously advantageous for the latitude error distribution; e.g., 98.82% of points have a latitude error of less than 6E-05 with the LRA-model, while the corresponding percentage with the HT-model is 78.82%.

4. Conclusion

This paper reports on a grid-based rapid numerical transformation model – a linear rule approximation model (LRA-model) for cylindrical projection transformation, which constructs linear polynomials to approximate the coordinate transformation and

uses a graticule to alleviate error propagation. Our experiments with simulated data demonstrate that the LRA-model, even though it cannot exclude systematic errors due to imperfections in defining the reference ellipsoid, exhibits high efficiency, high accuracy, and high stability and is simple and easy to use for both forward and inverse transformations. The LRA-model is appropriate for any area with mid or low latitudes, and the transformation error can be limited to meet the specific accuracy requirements by adjusting the interval distance of the graticule. Despite its lower exponent, the LRA-model exhibits advantages in calculation efficiency, accuracy and stability for coordinate transformations compared to the HT-model.

Our study does not involve azimuthal/conic projections or coordinate reference datum transformations. Therefore, further work will mainly focus on the applicability of the LRA-model to coordinate transformations with azimuthal / conic projections or changing reference datum and relevant uncertainties. All experiments are based on transformations between the WGS 84 Geographic Coordinate System (EPSG 4326) and the WGS 84 UTM ZONE 50N Plane Coordinate System (EPSG 32650), and we will test the accuracy and stability of the LRA-model using a map projection on a larger scale. Finally, because different coordinate transformation models exhibit advantages and weakness in terms of accuracy, the accuracy of the LRA-model can be improved by adopting the strong points of other models.

Acknowledgment

This paper is supported by Ministry of Land and Resources, Special Fund for Research in the Public Interest: Research on Efficient Identification and Integration Technologies of Arable Land Classification Monitoring. (Grant no. 201011006-4).

References

Behzad, B., et al., 2012. A Performance Profiling Strategy for High-performance Map Re-projection of Coarse-scale Spatial Raster Data[J]. In: Proceedings of Auto-Carto, Columbus, Ohio.

Jenny, Bernhard, et al., 2015. Real-time raster projection for web maps[J]. Int. J. Digit. Earth 41 (3), 1–14.

Bildirici, I.O., 2003. Numerical inverse transformation for map projections[J]. Comput. Geosci. 8, 1003–1011.

Bowring, B.R., 1990. The transverse mercator projection-a solution by complex numbers[J]. Surv. Rev. 237, 325–342.

Karney, Charles F.F., 2011. Transverse Mercator with an accuracy of a few nanometers[J]. J. Geod. 85 (8), 475–485.

Cromley, R.G., 1991. Digital cartography[M]. Prentice Hall, p. 317.

Engsager, K.E., et al., 2007. A highly accurate world wide algorithm for the transverse Mercator mapping (almost). In: Proceedings of XXIII international cartographic conference (ICC2007), Moscow.

Finn, M.P., et al., 2012. A program for handling map projections of small scale geospatial raster data[J]. Cartogr. Perspect. 71 (71), 53–67.

Hardy, R.L., 1990. Theory and applications of the multiquadric-biharmonic method [J]. Comput. Math. Appl. 19 (8), 163–208.

Ipbuker, C., 2002. An inverse solution to the Winkel Tripel Projection using partial derivatives[J]. Cartogr. Geogr. Inf. Sci. 29 (1), 37–42.

Junhua, T.E.N.G., et al., 2004. A new algorithm for map projection reverse transformation[J]. Acta Geod. Cartogr. Sin. 2, 179–185.

Liucheng, R.E.N., 2013. Searching for the transformation of map projection based on the differential theory of operator and inversion method[J]. J. Geomat. Sci. Technol. (1), 15–18.

Ozaki, R., et al., 2005. A fast method for coordinate calculation in projective transformations[J]. Trans. Inst. Electron. Inf. Commun. Eng. 2, 1–7.

Qi, ZHAO, et al., 2002. Study on the rapid algorithm of raster map projection transformation[J]. In: Proceedings of the 2nd International Conference on Image and Graphics, HEFEI, PEOPLES R CHINA, 4875, pp.154–159.

Weixin, S.U.N., et al., 2013. Analysis of numerical transformation of Gauss Kruger projection reverse transformation[J]. Eng. Surv. Mapp. 22 (3), 28–31.

Xie, Y., et al., 2011. Multi-rank method-achieving projection transformation with adjustable accuracy and speed[J]. In: ISPRS Workshop on High-Resolution Earth Imaging for Geospatial Information, Hannover, Germany.

Yang, Q., Snyder, J.P., 2000. Tobler W. Map Projection Transformation Principles and Applications [M]. Taylor & Francis, London.

Zhizhuo, W.A.N.G., 1990. Principle of photogrammetry[M]. Surveying and Mapping Press, Beijing, p. 145, in Chinese.

Zhongming, Z.H.A.O., et al., 2013. Spatial Information Technology Principles and Applications Part 1[M]. Science Press, Beijing, pp. 20–45, in Chinese.